半　导　体　学　报
JOURNAL OF SEMICONDUCTORS

Low-Temperature Growth and Photoluminescence of SnO_2 Nanowires*

Wang Bing[1,†], Xu Ping[1], and Yang Guowei[2]

(1 *Shenzhen Key Laboratory of Micro-Nano Photonic Information Technology, School of Electronic Science and Technology, Shenzhen University, Shenzhen　518060, China*)

(2 *State Key Laboratory of Optoelectronic Materials and Technologies, Institute of Optoelectronic and Functional Composite Materials, School of Physics Science & Engineering, Zhongshan University, Guangzhou　510275, China*)

Abstract: SnO_2 nanowires with a diameter of 25nm are synthesized at 550℃ by Au-Ag catalyst assisted thermal evaporation of SnO powders. The room-temperature photoluminescence spectra (PL) of the prepared nanowires are measured. Among the four PL peaks, the peak of 418nm is newly observed. This peak is caused by the plane defects of the twinned crystal nanowires. The formation of SnO_2 nanowires at low temperature is pursued on the basis of the VLS mechanism and application of the reaction source of SnO. We suggest that the chemical reactions of the low temperature and low concentration of the vaporized species are responsible for the thinner size of the SnO_2 nanowires.

Key words: crystal growth; nanomaterials; morphology; photoluminescence

EEACC: 0500; 0590

CLC number: TB303　　**Document code**: A　　**Article ID**: 0253-4177(2008)08-1469-06

1　Introduction

Nanoscale materials span a wide range of applications in nanoelectronic devices such as logic gate circuits[1], photodiodes[2], field emission sources[3], and gas storage materials[4] due to their nanometer-sized geometry and particular characteristics. Among these materials, SnO_2 with a wide band gap of 3.62eV at 300K has been utilized extensively in resistors, transistors, solar cell, antistatic coating, transparent heating elements, transparent conducting coating of glass, electrochemical modifiers on electrodes, electrodes in glass melting furnaces, special coating for energy-covering "low-emissivity" windows, and gas sensors to detect the leakage of reducing gases such as H, S, and CO[5~13]. However, realizing low temperature growth of SnO_2 nanostructures is one of critical issues in the field of device applications and many researchers are trying to achieve this goal[14~24]. For instance, various SnO_2 nanostructures have been synthesized by thermal evaporation in the temperature range of 1350 ~ 680℃. Among these methods, the lowest growth temperature of SnO_2 nanostructures by thermal evaporation is 680℃[24]. In this study, we prepare SnO_2 nanowires at 550℃. To the best of our knowledge, 550℃ is the lowest growth temperature of SnO_2 nanostructures by thermal evaporation among the reported studies so far[24].

2　Experiment

The SnO_2 nanowire synthesis is depicted below in detail. The schematic diagram of our apparatus used in the experiment is shown in Fig. 1. SnO powders (99.99%) were placed into a small quartz tube with an inner diameter of 15mm. An Au-Ag (atom ratio 1∶1) layer (about 7nm in thickness) was deposited on single crystal silicon (001) substrates with an area of $5mm^2$ by sputtering. The Au-Ag alloying target was employed in sputtering because the cost of the Au-Ag alloy is lower than that of pure gold. Next, Si substrates covered by Au-Ag alloy were put on the center of a ceramic plate near the source of the SnO powders inside the small quartz tube. Following this, the small quartz tube with an inner diameter of 15mm was pulled into the center of a large horizontal quartz tube with an inner diameter of 6cm that was inserted in a horizontal tube electric furnace. The whole system was evacuated by a vacuum pump for 20min, and then, the argon gas was guided into the system at 30sccm under a pressure of 2.6664×10^4 Pa. Afterwards, the furnace was rapidly heated up to 650℃ from room temperature and it remained at this temperature for 2.5h. The furnace temperature was measured by the thermal couple 1 in Fig. 1.

Meanwhile, the source temperature was 620℃ measured by the thermal couple 2, and the substrate temperature was 550℃ measured by the thermal cou-

* Project supported by the Scientific Research Foundation of Shenzhen University (No. 200839)

† Corresponding author. Email: wangbing@szu.edu.cn755-2653-4860

Received 12 May 2008, revised manuscript received 19 June 2008

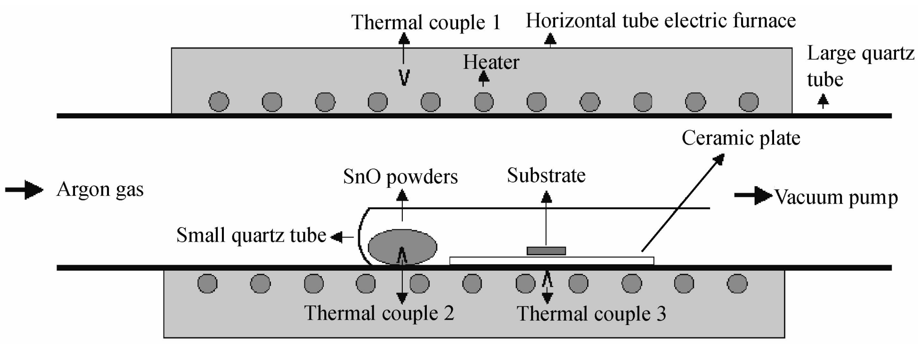

Fig. 1 Schematic diagram of the apparatus used in the experiment

ple 3. In our case, the temperature of thermal couple 3, 550℃, is the growth temperature. Finally, the system was cooled to room temperature over several hours. We found that a lay of gray-blue production was deposited on Si substrates. The morphology and microstructure of the products were analyzed by scanning electron microscopy (SEM) and field emission scanning electron microscopy (FESEM). The structure of the products was analyzed using X-ray diffraction (XRD) and Raman spectrometer (Raman) at room temperature. PL measurement was performed at room temperature using a laser line of 265nm as the excitation source.

3 Results and discussion

SEM patterns and the low magnified FESEM image of the prepared nanowires are displayed in Fig. 2, and the corresponding high magnified FESEM image of these nanowires are displayed in Fig. 3 (a). The nanowires with a diameter of 25nm are well-distributed. The FESEM image of SnO_2 nanowires synthesized at 950℃ is also shown in Fig. 3 (b)[25]. The diameter of the SnO_2 nanowires (950℃) is about 100nm, and larger than that of the SnO_2 nanowires (550℃) in Fig. 3(a). The corresponding XRD pattern shown in Fig. 2 (c) from the as-synthesized products can be indexed according to the tetragonal rutile structure of SnO_2 with lattice constants of $a = 0.4738$nm and $c = 0.3188$nm, which is consistent with the standard values of bulk SnO_2 (JCPDS 21-1250). Rutile SnO_2 belongs to the space group D_{4h}^{14}, of which the normal lattice vibration at the Γ point of the Brillouin zone is given on the basis of group theory[26]: $\Gamma = 1A_{1g} + 1A_{2g} + 1A_{2u} + 1B_{1g} + 1B_{2g} + 2B_{1u} + 1E_g + 3E_u$. Among them, the four first order active Raman modes are B_{1g}, E_g, A_{1g}, and B_{2g}, and the active IR modes are A_{2u}, E_u, and B_{1u}. In the room temperature Raman scattering spectra (Fig. 2 (d)) of the SnO_2 nanowires, three fundamental Raman peaks at 474, 630, and 772cm^{-1} are displayed, which separately correspond to the E_g, A_{1g}, and B_{2g} vibration modes[27]. Thus, these peaks further confirm that the as-synthesized SnO_2 nanowires possess the characteristic of the tetragonal rutile structure. In addition, the two weak Raman bands of 497 and 696cm^{-1} seem to correspond to IR-active A_{2u} TO and A_{2u} LO modes (LO is the mode of the longitudinal optical photos and TO is the mode of the transverse optical photos). This correspondence is similar to $E_{u(2)}$ TO of SnO_2 nanopowders and $E_{u(2)}$ LO of SnO_2 nanorods[17,18,28]. Furthermore, the peak at 540cm^{-1} has not been reported in the Raman study of SnO_2 nanowires. We identify it as S_2 mode, which is believed to be the consequence of the disorder activation of SnO_2 nanowires[23]. Finally, the peak at 520cm^{-1} is the characteristic peak of the Si substrate.

The TEM results and the EDS spectrum of the synthesized SnO_2 nanowire are shown in Fig. 4. The TEM bright field image of the tip with the size of 25nm growing at the end of the nanowire with a diameter of 20nm is displayed in Fig. 4(a). The EDS spectrum in Fig. 4(b) recorded along the nanowire indicated that the nanowire is composed of Sn and O, and Cu comes from the TEM grid. The EDS spectrum in Fig. 4(c) recorded at the tip indicates that the tip is composed of Au and Sn, and Cu comes from the TEM grid. The HRTEM image of the nanowire shown in Fig. 4(d) indicates that the interplanar spacing of 0.334nm corresponds to the crystallographic planes of (110), and the SAED pattern in Fig. 4(e) recorded with the electron beam perpendicular to the long axis of the nanowire indicates that the growth direction of the nanowire is along [1$\bar{2}$1].

Interestingly, we observed twinned crystal in the synthesized nanowires shown in Fig. 5. The TEM bright field image of a twinned crystal nanowire with the diameter of 20nm is displayed in Fig. 5(a), and the corresponding HRTEM image and SAED pattern are shown in Figs. 5(b) and 5(c). The "twin" parts are indexed with a subscript "T" and the remaining matrix part indices are marked without subscript in Figs. 5 (a) and 5(c). The HRTEM shown in Fig. 5(b)

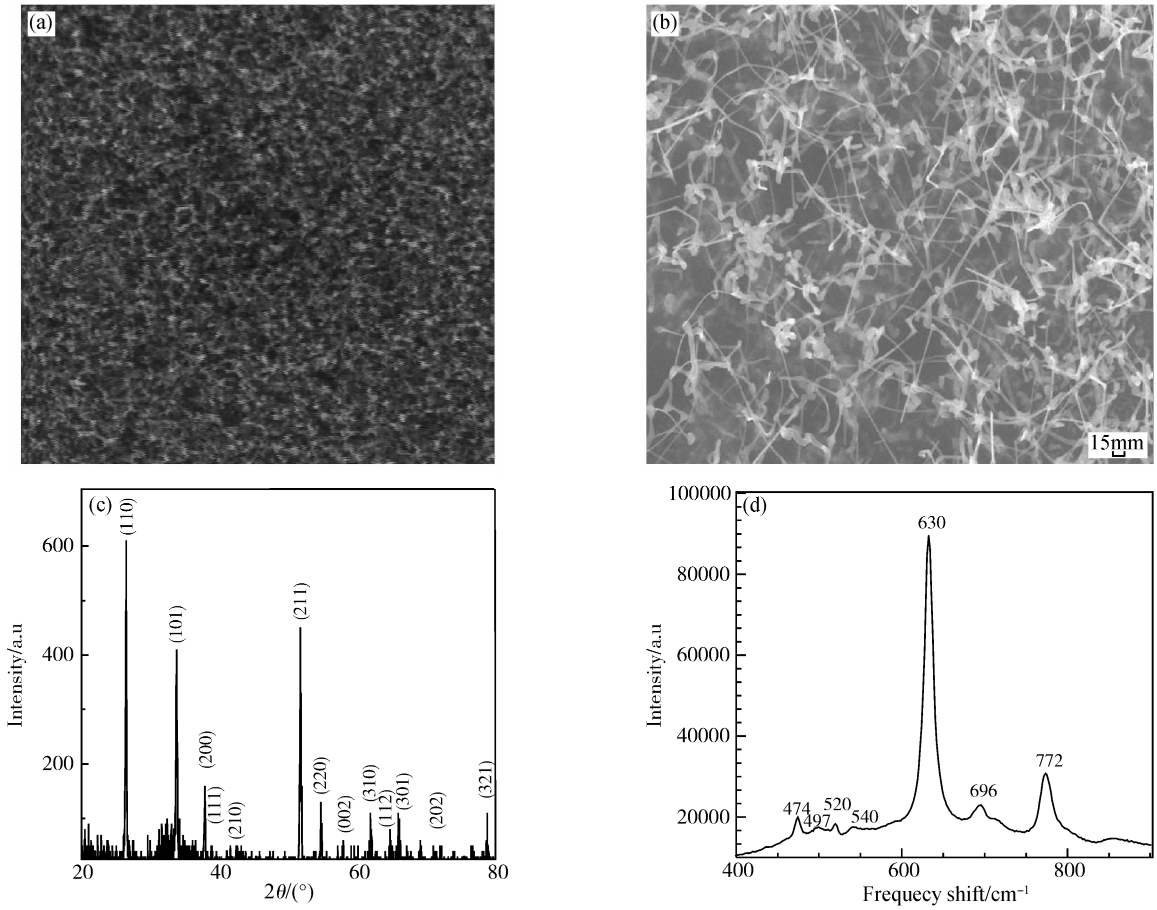

Fig.2　SEM morphology (a), low magnified FESEM morphology (b), XRD pattern (c), and Raman spectrum (d) of the synthesized SnO_2 nanowires

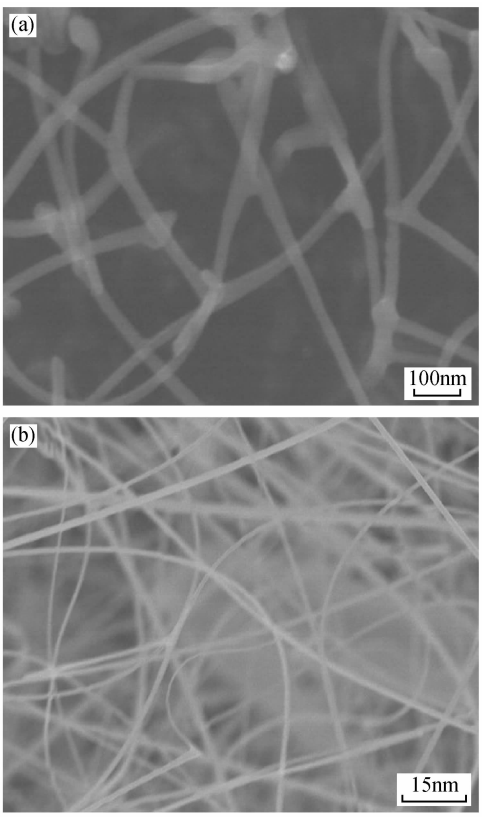

Fig.3　Highly magnified FESEM morphologies of the SnO_2 nanowires synthesized at 550℃ (a) and 950℃ (b)

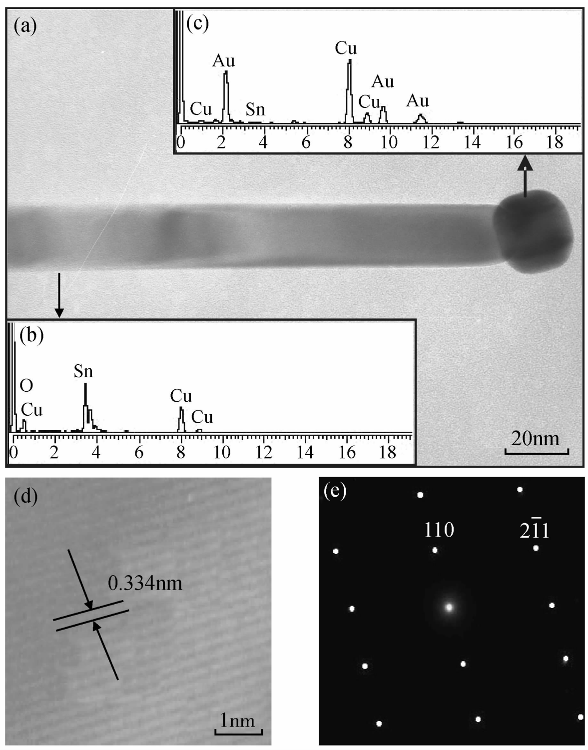

Fig.4　(a) TEM bright field image of a nanowire with the tip; (b) EDS spectrum of the nanowire; (c) EDS spectrum of the tip; (d) HRTEM image of the nanowire; (e) Corresponding SAED pattern of the nanowire with an electron beam along the [1$\bar{1}\bar{3}$] direction

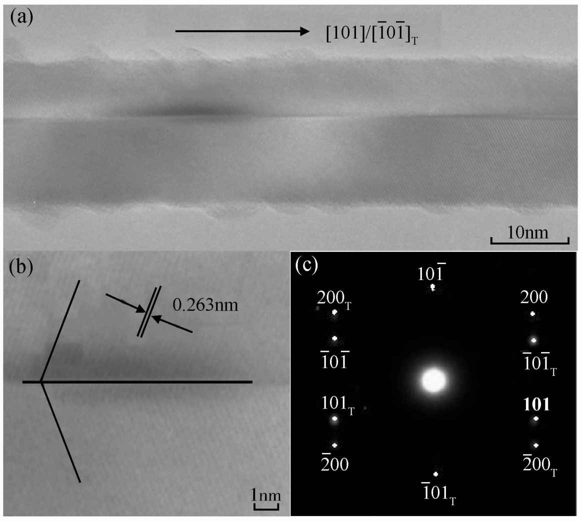

Fig. 5 TEM bright field image (a), HRTEM image (b), and SAED pattern (c) of a twinned crystal nanowire

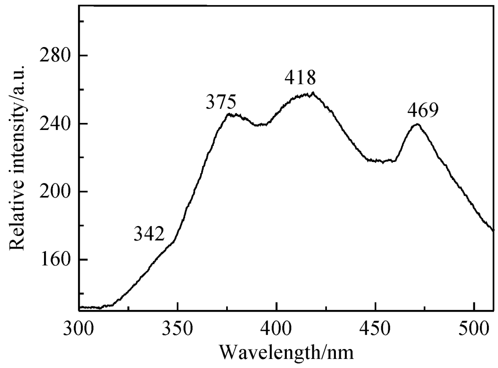

Fig. 6 Room temperature PL spectrum of the synthesized SnO_2 nanowires

indicates that the interplanar spacing of 0.263nm corresponds to the crystallographic planes of (101) and $(101)_T$. The electron beam is along the [010] direction of the SnO_2 rutile structure in Fig. 5(c). The twinning plane is $(10\bar{1})$ and the twinned direction is $[\bar{1}0\bar{1}]_T$, parallel to the growth direction of the SnO_2 nanowire [101]. We suggest that the twin formation can be explained by regarding the twin as one part of the crystal (twin) rotated 180° along the $(10\bar{1})$ crystal plane, while the remaining parts of the crystal (matrix) retain the original direction[29]. This twinned crystal structure is a kind of plane defect of crystal.

The photoluminescence of the obtained SnO_2 nanowires was investigated at room temperature and the result is shown in Fig. 6. The PL spectra consist of a weak emission band at 342nm and three sharp and strong emission band located at 375, 418, and 469nm. First, the peak at 342nm is the band-to-band emission peak of the SnO_2 nanowires, which originates from the recombination of the electron-hole[30]. This peak is weaker than the other three peaks because the peaks caused by defects or nanocrystal grains or defect levels associated with oxygen vacancies or tin interstitials resulting from the size effect of the SnO_2 nanowires is strong so as to cripple the band-to-band emission peak[31]. Second, the 375nm peak is attributed to the band-to-acceptor peak and related to the impurity or defect concentration and not to the structural properties[32]. Third, the peak at 469nm is possibly attributed to electron transition mediated by defects levels such as oxygen vacancies in the band gap[33]. Finally, the peak at 418nm is newly observed and is possibly caused by the plane defects of the twinned crystal nanowires shown in Fig. 5.

The mechanism of the low temperature growth of SnO_2 nanowires can be explained on the basis of the vapor-liquid-solid (VLS) processes. In experiment, Au as a catalyst is usually used to assist the SnO_2 nanowires synthesis, which is demonstrated by the Au existing in the tip detected by the EDS spectrum in Fig. 4(e). During the thermal evaporation process, the following chemical reactions will occur above 300℃[24,34,35].

$$2SnO\,(s) = Sn\,(l) + SnO_2(S) \quad (1)$$

$$SnO_2(s) = SnO\,(g) + 1/2\,O_2 \quad (2)$$

Reaction (2) is reversible. A study of the VLS growth of SnO_2 whiskers under high temperature (1300℃) indicated that the Sn globule at the tip is essential for the VLS growth of SnO_2 whiskers[35]. In our experiment, Sn particles produced in reaction (1) are liquid at the reaction temperature because of the low melting point of 231.9℃, which seems to be one of the factors causing the low temperature growth of SnO_2 nanowires. On the other hand, the Sn droplets fell on the substrate covered by Au-Ag alloy and form Sn-Au alloying droplets by reacting with Au particles. Meanwhile, these alloying droplets can provide energetically favorable sites for the adsorption of oxygen and SnO vapor[23], which is also one of the key factors for the VLS growth of nanowires. The vaporized species, SnO and O_2, deposit on the surface of the Sn-Au alloying droplets and react with each other, forming SnO_2 that subsequently dissolves in the Sn droplets. The continuous dissolution of SnO_2 leads to a supersaturated solution. Ultimately, the SnO_2 nanowires grow by precipitation of SnO_2 from the supersaturated droplets[24]. The residual Sn is carried out by the flowing Argon gas.

The application of the reaction source of SnO powder is essential for the low temperature of the nanowires. For example, SnO_2 nanowires had been synthesized at 950℃ by thermal evaporation of active carbon and SnO_2 powders[25]. With the help of the active carbon, the growth temperature of the nanowires decreased to 950℃ because of the higher melting point of 1630～2000℃ for SnO_2. In our experiment, without the help of the active carbon, the growth temperature of the nanowires is only 550℃ because of lower melting point of 1040℃ and the unstable chemical characteristics lower than 1040℃ for SnO.

The low temperature and the concentration of vaporized species presumably play important roles in the growth of the thinner SnO_2 nanowires. At 550℃, with low pressure (2.6664×10^4 Pa) and low gas flow of rate (30sccm), the concentration of SnO and O_2 vapor are sufficient for the VLS growth of SnO_2 nanowires[24]. The theoretical and most stable crystal habit of SnO_2 is a tetragon elongated along the *c*-axis[36]. Accordingly, SnO_2 have first-optimized and second-optimized growth directions. At high temperatures and high concentrations, the single crystal grows along the two optimized directions simultaneously[36]. Moreover, the growth along the first-optimized direction is faster than along the second-optimized direction, so that products such as nanobelts can be formed. At low temperatures and low concentrations, the single crystal grows along one of the two optimized directions[36] to form SnO_2 nanowires in our experiment. The slight differences in temperature and concentration will influence the diameters of the nanowires. For example, at the low temperature of 550℃ under the low pressure (2.6664×10^4 Pa) and the low gas flow of rate (30sccm), the diameter of the synthesized SnO_2 nanowires (Fig. 3 (a)) is thinner than that of the SnO_2 nanowires produced at the high temperature of 950℃ (Fig. 3 (b)) under the high pressure (8.6658×10^4 Pa) and high gas flow of rate (300 sccm)[25]. Once the initial nucleation starts, the crystal grows in epitaxial ways, which results in the preferential orientation of SnO_2 lattice planes, forming SnO_2 nanowires.

4 Conclusion

In summary, SnO_2 nanowires had been synthesized at 550℃ with SnO powders by thermal evaporation. The room temperature photoluminescence spectrum of the prepared SnO_2 nanowires showed that the peak at 418nm is newly observed and is caused by the plane defects of the twinned crystal nanowires. The mechanism of the low temperature growth of SnO_2 nanowires had been explained based on the VLS process and application of the reaction source of SnO. We suggest that the chemical reactions of the low temperature and low concentration of the vaporized species are responsible for the thinner size of SnO_2 nanowires.

References

[1] Xia Younan, Yang Peidong, Sun Yugang, et al. one-dimensional nanostructures: synthesis, characterization, and applications. Adv Mater, 2003, 15: 353

[2] Wang Changchun, Guo Zhixin, Fu Shoukuan, et al. Polymers containing fullerene or carbon nanotube structures. Progress in Polymer Science, 2004, 29: 1079

[3] Nakamura S. The roles of structural imperfections in InGaN-based blue light-emitting diodes and laser diodes. Science, 1998, 281: 956

[4] Liu C, Fan Y Y, Liu M, et al. Hydrogen storage in single-walled carbon nanotubes at room temperature. Science, 1999, 286: 1127

[5] Ogawa H, Abe A, Nishikawa M, et al. Cobalt and nickel cations as corrosion inhibitors for galvanized steel. Journal of Electrochemical Society, 1981, 128: 2020

[6] Arfsten N J, Kaufmann R, Dislich H, et al. Ultrastructure processing of ceramics, glasses and composites. Proceedings of the International Conference on Ultrastructure Processing of Ceramics Glass and Composites, 1984

[7] Jarzebski Z M, Marton J P. Physical properties of SnO_2 materials. Journal of Electrochemical Society, 1976, 123: 299

[8] Whittingham M S. The role of ternary phases in cathode reactions. Journal of Electrochemical Society, 1976, 123: 333

[9] Wei P H, Li G B, Zhao S Y, et al. Gas-sensing properties of Th/SnO_2 thin-film gas sensor to trimethylamine. Journal of Electrochemical Society, 1999, 146: 3536

[10] Varol S H, Hinsch A. SnO_2: Sb dip coated films on anodized aluminum selective absorber plates. Solar Energy Mater and Solar Cells, 1996, 40: 273

[11] Kim T W, Liu D U, Lee J H, et al. Surface and microstructural properties of SnO_2 thin films grown on p-InP (100) substrates at low temperature. Solid State Commun, 2000, 115: 503

[12] Li G J, Zhang H, Kawi S, et al. Relationships between sensitivity, catalytic activity, and surface areas of SnO_2 gas sensors. Sensor Actuators B, 1999, 60: 64

[13] Leite E R, Weber I T, E Longo, et al. A new method to control particle size and particle size distribution of SnO_2 nanoparticles for gas sensor application. Adv Mater, 2000, 12: 965

[14] Pan Z W, Dai Z R, Wang Z L. Nanobelts of semiconducting oxides. Science, 2001, 291: 1947

[15] Dai Z R, Gole J L, Stout J D, et al. Tin oxide nanowires, nanoribbons, and nanotubes. Journal of Physical Chemistry B, 2002, 106: 1274

[16] Hu J Q, Ma X L, Shang N G, et al. Large scale rapid oxidation synthesis of SnO_2 nanoribbons. Journal of Physical Chemistry B, 2002, 106: 3823

[17] Peng X S, Zhang L D, Meng G W, et al. Micro-Raman and infrared properties of tin oxide nanobelts synthesized from tin metal and SiO_2 powders. J Appl Phys, 2003, 93: 1760

[18] Liu Y K, Zheng C L, Wang W Z, et al. Synthesis and characterization of rutile SnO_2 nanorods. Adv Mater, 2001, 13: 1883

[19] Zhang J, Jiang F H, Zhang L D, et al. Synthesis of SnO_2 nanobelts and their structural characterization. J Phys D: Appl Phys, 2003, 36: 21

[20] Wang B, Yang Y H, Wang C X, et al. Growth and photoluminescence of SnO_2 nanostructures synthesized by Au-Ag alloying catalyst assisted carbothermal evaporation. Chemical Physics Letters, 2005, 407: 347

[21] Wang Y, Lee J, Deivaraj T C. Controlled synthesis of V-shaped SnO_2 nanorods. Journal of Physical Chemistry B, 2004, 108: 13589

[22] Sun S H, Meng G W, Gao T, et al. Large-scale synthesis of SnO_2 nanobelts. Appl Phys A, 2003, 76: 287

[23] Wang J X, Liu D F, Yan X Q, et al. Growth of SnO_2 nanowires

with uniform branched structures. Solid State Commun, 2004, 130:89
[24] Chen Y Q, Cui X F, Zhang K, et al. Bulk-quantity synthesis and self-catalytic VLS growth of SnO_2 nanowires by lower-temperature evaporation. Chemical Physics Letters, 2003, 369:16
[25] Wang B, Yang Y H, Wang C X, et al. Nanostructures and self-catalyzed growth of SnO_2. J Appl Phys, 2005, 98:073520
[26] Porto S P S, Fleury P A, Damen T C, et al. Ramen spectra of TiO_2, MgF_2, ZnF_2, FeF_2, and MnFZ. Phys Rev, 1967, 154:522
[27] Sun S H, Meng G W, Zhang G X, et al. Raman scattering study of rutile SnO_2 nanobelts synthesized by thermal evaporation of Sn powders. Chemical Physics Letters, 2003, 376:103
[28] Abello L, Bochu B, Gaskov A, et al. Structural Characterization of nanocrystalline SnO_2 by X-ray and Raman spectroscopy. Journal of Solid State Chemistry, 1998, 135:78
[29] Dai Z R, Gole J L, Wang Z L, et al. Tin oxide nanowires, nanoribbons, and nanotubes. Journal of Physical Chemistry B, 2002, 106:1274
[30] Lee E J H, Ribeiro C, Giraldi T R, et al. Photoluminescence in quantum-confined SnO_2 nanocrystals: evidence of free exciton decay. Appl Phys Lett, 2004, 84:1745
[31] Kimand T W, Lee D U. Microstructural, electrical, and optical properties of SnO_2 nanocrystalline thin films grown on InP (100) substrates for applications as gas sensor devices. J Appl Phys, 2000, 88:3759
[32] Jeong J, Choi S, Chang C, et al. Photoluminescence properties of SnO_2 thin films grown by thermal CVD. Solid State Commun, 2003, 127:595
[33] Gu F, Wang S F, Lu M K, et al. Photoluminescence properties of SnO_2 nanoparticles synthesized by sol-gel method. Journal of Physical Chemistry B, 2004, 108:8119
[34] Moreno M S, Mercader R C, Bibiloni A G, et al. Study of intermediate oxide in SnO thermal decomposition. Journal of Physical Condens Matter, 1992, 4:351
[35] Nagano M. Growth of SnO_2 whiskers by VLS mechanism. J Cryst Growth, 1984, 66:377
[36] Sun S H, Meng G W, Zhang M G, et al. Synthesis of SnO_2 nanostructures by carbon thermal reduction of SnO_2 powder. J Phys D: Appl Phys, 2004, 37:409

SnO_2 纳米线的低温生长及光致发光研究*

王 冰[1,†] 徐 平[1] 杨国伟[2]

(1 深圳大学电子科学与技术学院 深圳微纳光子信息技术重点实验室，深圳 518060)
(2 中山大学光电材料与技术国家重点实验室，广州 510275)

摘要： 在550℃下，通过Au-Ag合金助催热蒸发氧化亚锡，制备了25nm的SnO_2纳米线.测试了SnO_2纳米线的室温光致发光谱，其四个发光峰中，418nm的峰是新发现的峰，它是孪晶纳米线的面缺陷造成的.SnO_2纳米线的低温生长机制遵从VLS生长机制，且与SnO粉末的应用有一定的关系.SnO_2纳米线的较小尺度与气相因子的低温度低浓度化学反应有关.

关键词： 晶体生长；纳米材料；形貌；光致发光
EEACC： 0500；0590
中图分类号： TB303 **文献标识码：** A **文章编号：** 0253-4177(2008)08-1469-06

* 深圳大学科研启动基金资助项目(批准号:200839)
† 通信作者.Email:wangbing@szu.edu.cn
2008-05-12收到，2008-06-19定稿